

Received: 2020.03.26

Accepted: 2020.04.22

Available online: 2020.04.30

Published: 2020.05.08

# Differential Metabolic Pathways and Metabolites in a C57BL/6J Mouse Model of Alcoholic Liver Disease

Authors' Contribution:

Study Design A

Data Collection B

Statistical Analysis C

Data Interpretation D

Manuscript Preparation E

Literature Search F

Funds Collection G

ABCE 1 **Tai Ma\***

ABCD 1 **Yue Li\***

ABC 2 **Yun Zhu**

ABD 1 **Shuling Jiang**

BC 1 **Chen Cheng**

AD 2 **Zhiwei Peng**

G 1 **Long Xu**

1 School of Basic Medical Science, Anhui Medical University, Hefei, Anhui, P.R. China

2 The First Affiliated Hospital of Anhui Medical University, Hefei, Anhui, P.R. China

\* Tai Ma and Yue Li contributed equally

**Corresponding Author:** Long Xu, e-mail: [xulong@ahmu.edu.cn](mailto:xulong@ahmu.edu.cn)

**Source of support:**

The present study was supported by the National Natural Science Foundation of China [81873570] and grants for the 4<sup>th</sup> Excellent Scientific Research of QNBJRC from Anhui Medical University [2013500023]. This study was carried out at the Basic SPF Animal Laboratory of Anhui Medical University. Animal ethics approval number: LLSC20180145

**Background:** Alcoholic liver disease (ALD), an important cause of acute or chronic liver injury, results from binge drinking or long-term alcohol consumption. To date, there is no well-established mouse model with a comprehensive metabolic profile that mimics ALD in humans. This study aimed to explore the differential metabolic pathways and related differential metabolites in the liver of an ALD mouse model.


**Material/Methods:** A C57BL/6J mouse model of ALD was induced by alcohol feeding for 10 days plus binge alcohol feeding. The metabolomic profiles in the liver of the ALD mouse model was detected through ultra-high-pressure liquid chromatography-quadrupole time-of-flight tandem mass spectrometry (UHPLC/Q-TOF-MS).

**Results:** A total 35 metabolites were significantly altered during the development of ALD. These metabolites were correlated to multiple metabolic pathways, including purine metabolism, the pentose phosphate pathway, cysteine and methionine metabolism, D-glutamine and D-glutamate metabolism, pyrimidine metabolism, and vitamin B6 metabolism.

**Conclusions:** The findings of the present study reveal potential biomarkers of ALD, and provide further insights into the pathogenesis of ALD.

**MeSH Keywords:** **Lipid Metabolism Disorders • Liver Diseases, Alcoholic • Metabolomics**

**Full-text PDF:** <https://www.medscimonit.com/abstract/index/idArt/924602>

 2513

 2

 8

 32



## Background

Alcohol consumption, both binge and chronic, is a major health problem worldwide, and it is often accompanied by significant socioeconomic burdens. Excessive intake of alcohol leads to alcoholic liver diseases (ALD), which comprises a range of disorders, including fibrosis, hepatosteatosis, alcoholic hepatitis, cirrhosis, and hepatocellular carcinoma. The development of such conditions is mainly due to the generation of alcohol-induced metabolic factors that cause lipid metabolism disorder, hepatocyte apoptosis and regeneration, oxidative stress, collagen deposition, and dysregulation of the hepatic immune response [1]. Nevertheless, the metabolic mechanisms involved in the progression of ALD remain to be clarified.

Metabolomics is an emerging platform for the quantitative and qualitative analysis of endogenous metabolites and for exploring the potential mechanism involved in certain diseases [2]. The overall function of biological systems can be understood by detecting changes in metabolites. Therefore, the diagnosis and treatment of diseases based on changes in metabolites have gradually become more widespread in clinical practice. Modern analytical techniques, such as ultra-high-performance liquid chromatography (UHPLC), gas chromatography (GC), and capillary electrophoresis (CE), combined with high-resolution mass spectrometry (HRMS) and proton nuclear magnetic resonance (<sup>1</sup>H-NMR), have recently been introduced for metabolomics analysis [3].

Although metabolomic profiling has been carried out to identify potential metabolic pathways involved in mouse or rat models of ALD, only feces or urine samples have been used for detection [4,5]. There is still a need to further identify more key metabolites involved in the development and progression of ALD using liver samples of an appropriate animal model.

In the present study, UHPLC coupled with quadrupole time-of-flight mass spectrometry (Q-TOF-MS) and liquid chromatography-mass spectrometry (LC-MS) platform-based metabolomics was applied for analyzing the liver metabolic profiles in the Gao-Binge alcoholic C57BL/6J mouse model [6]. After feeding with alcohol for 10 days plus binge feeding of alcohol, 35 metabolites were significantly changed, and 6 related metabolic pathways were examined. These findings could aid in investigations of the metabolic mechanisms underlying the development of ALD in humans.

## Material and Methods

### Animal and alcohol feeding model

Male C57BL/6 mice (5–6 weeks old) were acquired from Slack Laboratory Animals Co. (Shanghai, China). The mice were

housed under specific pathogen-free conditions and handled based on the instructions described in the Guide for the Care and Use of Laboratory Animals. This study was carried out at the Basic SPF Animal Laboratory of Anhui Medical University. The study procedures were approved by the Animal Ethics Committee of Anhui Medical University (approval number: LLSC20180145). Eight-week-old C57BL/6 mice were fed an ethanol-containing Lieber-Decarli liquid diet or an isocaloric control diet to study ALD, as previously described [6].

### Measurement of liver injury or steatosis

The serum concentrations of aspartate aminotransferase (AST) and alanine aminotransferase (ALT) were detected using commercial kits from Nanjing Jian Cheng Bioengineering Institute (Nanjing, China). Commercial kits for triglyceride (TG) quantification were obtained from Beijing Applygen Institute (Beijing, China). Liver tissue was collected at 9 h after gavage with alcohol. Paraffin-embedded sections were processed for hematoxylin-eosin (HE) staining, and frozen sections were stained with Oil Red O for hepatic steatosis evaluation.

### LC-MS/MS analysis

A combination of UPLC BEH Amide columns using the UHPLC system and the Triple TOF 6600 system was applied in LC-MS/MS analysis. The conditions for pre-installed ESI source were as follows: ion source gas 1 was 60 psi, ion source gas 2 was 60 psi, curtain gas was 35 psi, source temperature was 650°C, and ion spray voltage float (ISVF) was positive or negative voltage 5000 V or –4000 V. In this study, according to the *t* test, *P* value <0.05 denoted statistical significance, and the first major component of the OPLS-DA model had a variable importance in the projection (VIP) higher than 1. The metabolomic analysis process of the liver is shown in Figure 1. We performed statistical analysis of all data, with screening based on qualitative and (relative) quantification of metabolites, normalization and standardization, for quantitative information used for statistical analysis. The *t* test was used for univariate statistical analysis, and PCA and OPLS-DA were used for multivariate statistical analysis to screen out significantly different metabolites. Then, the correlation analysis of advanced data and metabolic pathway analysis of optional data were conducted.

### Statistical analyses

Biochemical parameters with normal distribution were described as the mean±standard deviation (SD). The differences of these parameters were evaluated by GraphPad Prism 6.0 software (La Jolla, CA, USA), and *P*<0.05 denoted statistical significance.

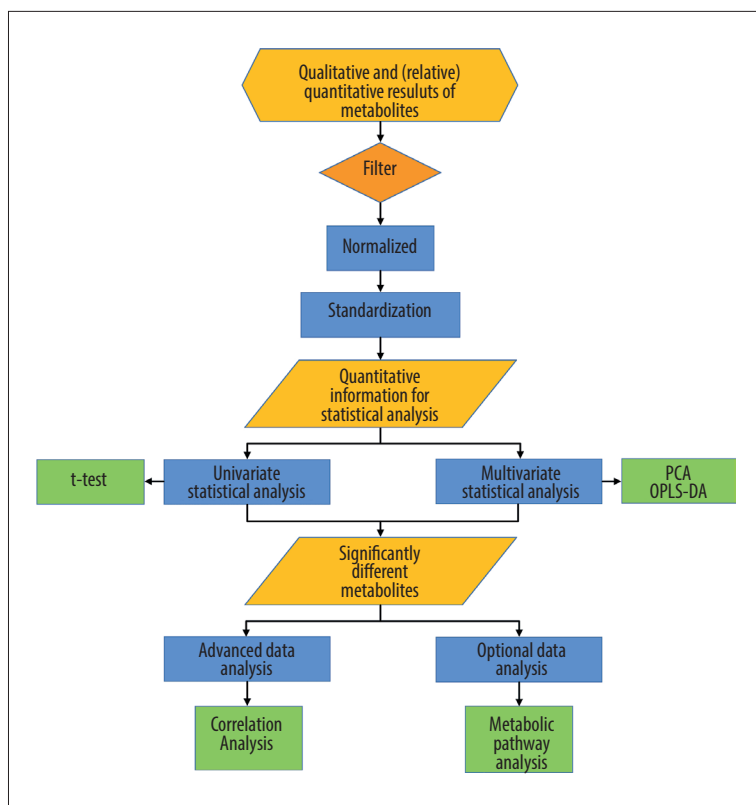


**Figure 1.** The metabolomic analysis process of the liver.

## Results

### Establishment of the ALD model in male C57BL/6J mice

In comparison with mice fed a control liquid diet, mice fed an alcohol diet developed more severe liver injury, as demonstrated by higher levels of ALT and AST (Figure 2A, 2B), increased hepatic steatosis, and higher levels of TG and HE or Oil Red O staining (Figure 2C–2E). Additionally, compared with the mice fed the control diet, mice fed alcohol exhibited more severe liver inflammation and higher expression levels of mRNA that encode inflammatory cytokines (Figure 2F, 2G). The weight change ratio of mice is shown in Figure 2H, in which the alcohol-fed mice lost weight compared to the control group. Thus, the ALD mouse model was considered a viable model.

### Stability analysis of UPLC/Q-TOFMS system

The assured UHPLC/Q-TOF-MS quality control (QC) samples were used for profiling the metabolomes of liver samples from control diet-fed and ethanol-fed mice, which were assessed regularly (every 6 samples) throughout the experiment to detect system stability under positive mode and negative mode. The quality control samples were collected and the alcohol group was separated from control group. The stability and reliability of UHPLC/Q-TOF-MS analysis were verified (Figure 3A, 3B). Due to the insufficiency of visual inspection for

separating groups, pattern recognition was applied to visually differentiate intergroup differences in metabolites.

### Separation between experimental group and control group

A comparison between the control diet-fed group and ethanol-fed group was performed using multivariate statistical analysis to examine clusters for each group, including principal component analysis (PCA) and orthogonal partial least-squares discrimination analysis (OPLS-DA) techniques. PCA is a statistical method for comparing possibly related variables that converts variables to linearly uncorrelated variables (principal components) by orthogonal transformation [7]. The PCA score map showed that all samples were within the 95% confidence interval (Figure 4A, 4B), achieving good separation between the control group and experimental group.

### Changes in liver biochemical metabolites in alcohol model mice

To acquire more reliable meta-group differences and group relevance information, the orthogonal variables in metabolites were percolated through the OPLS-DA analysis, which were not associated with the categorical variables, and the non-orthogonal variables and orthogonal variables were analyzed separately [8]. OPLS-DA score chart illustrated that the differences between 2 groups of samples were statistically significant (Hotelling's

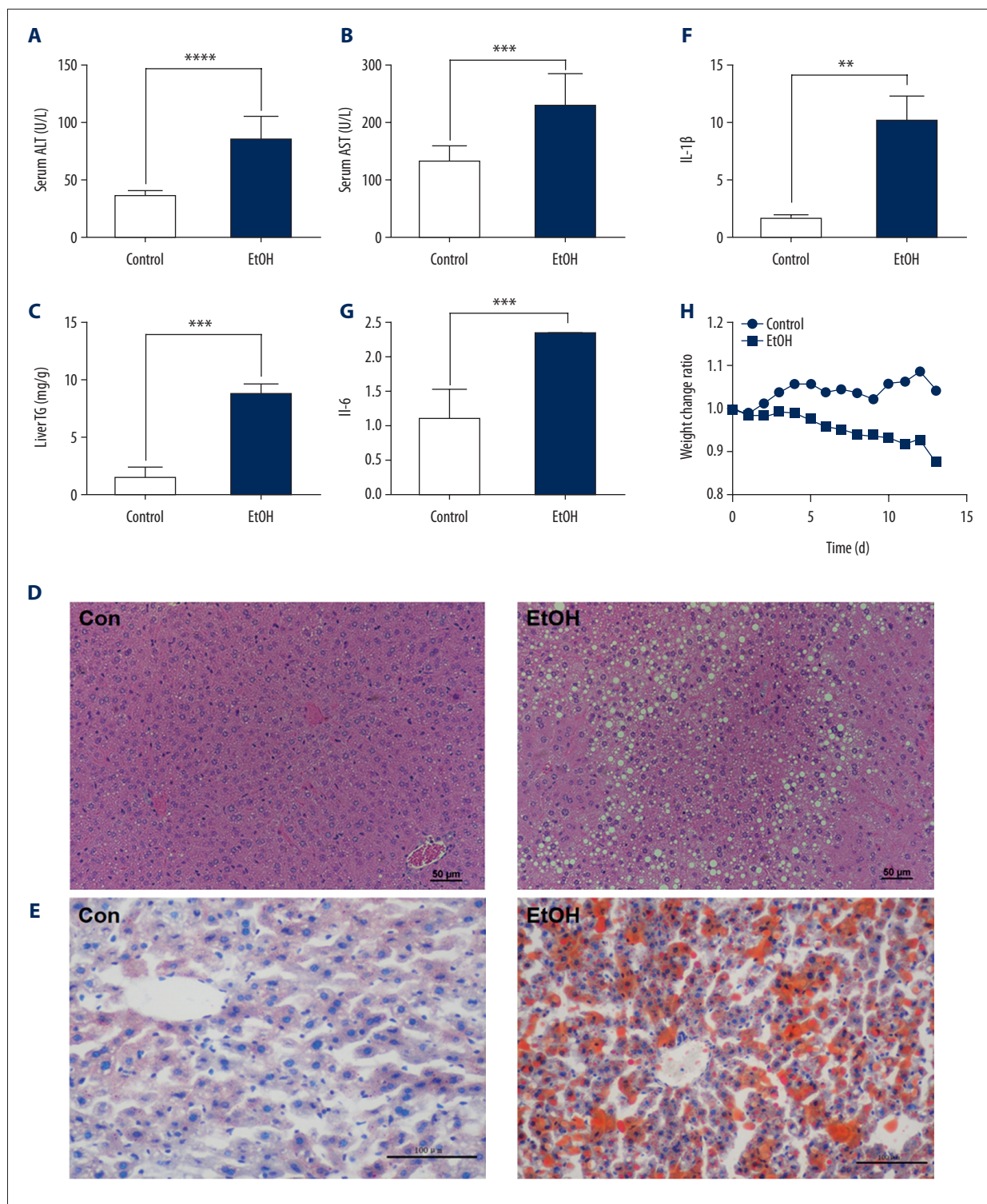


**Figure 2.** C57BL/6 mouse feeding control and ethanol-fed for 10 consecutive days. The mice were euthanized 9 h after gavage. (A, B) Serum ALT and AST levels; (C) Mouse liver TG levels; (D) Liver tissue HE and (E) Oil Red O staining (original magnification, 200×); (F) Inflammation indicator IL-1 $\beta$  level; (G) Inflammation indicator IL-6 level. (H) Weight change ratio of mice. Significance is designated by symbols that do not share a common symbol and are significantly different from each other at  $P < 0.01$ . Significance is designated by asterisks with \*  $P < 0.05$ ; \*\*  $P < 0.01$ ; \*\*\*  $P < 0.001$ ; \*\*\*\*  $P < 0.0001$ .

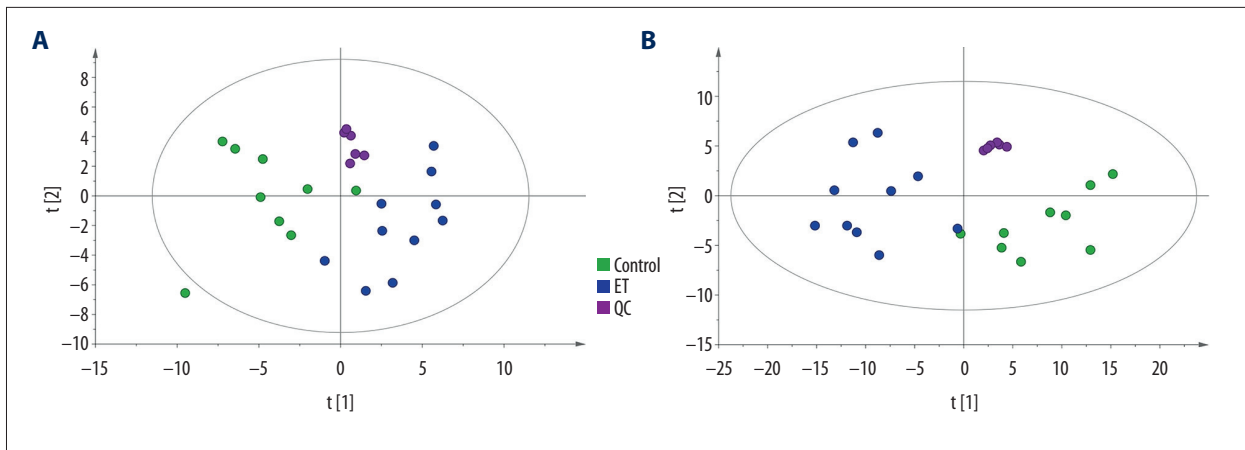


**Figure 3.** Positive ion PCA of all QC samples (A) and Negative ion PCA of all QC samples(B). Con (Control, fed isocaloric control diet), ET (EtOH, fed an ethanol-containing Lieber-DeCarli liquid diet), QC (Quality control, performed for profiling the metabolomes of liver samples from pair-fed and ethanol-fed mice).

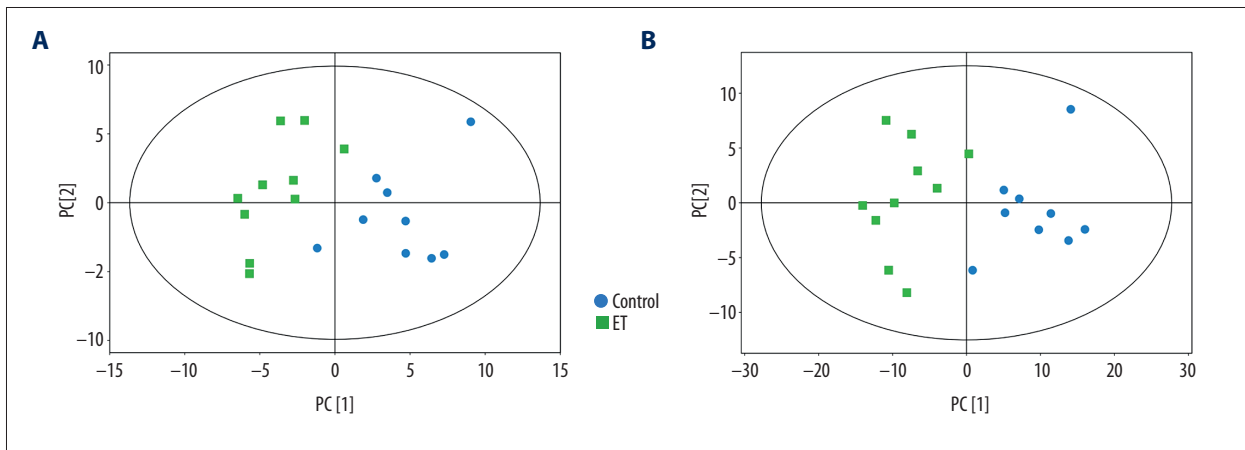


**Figure 4.** Score scatter plot of PCA model for group ET (EtOH) vs. Con (Control) in POS (A) and NEG (B).

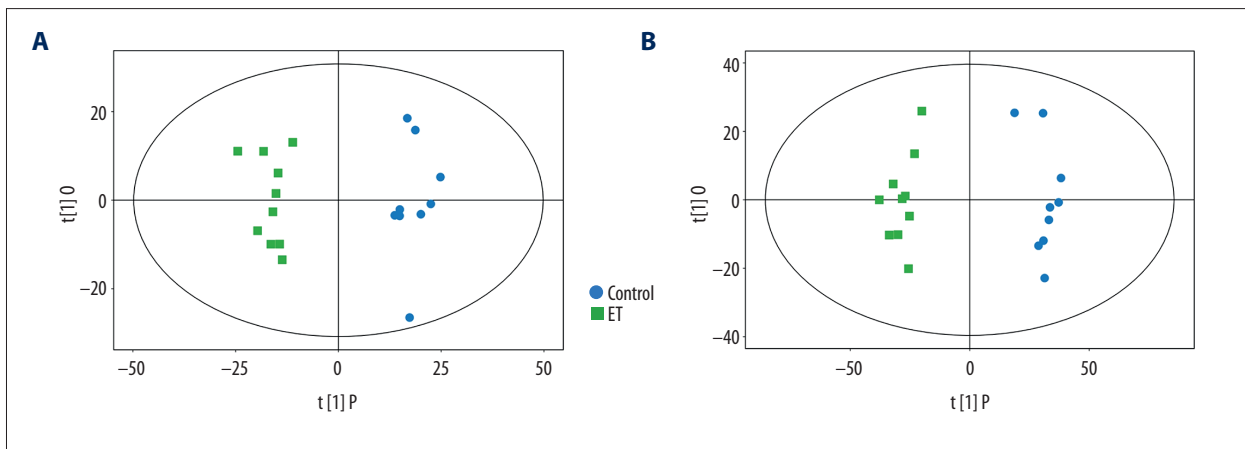


**Figure 5.** Orthogonal partial least-squares discriminant analysis (OPLS-DA) score map of ET (EtOH) vs. Con (Control) in POS (A) and NEG (B).

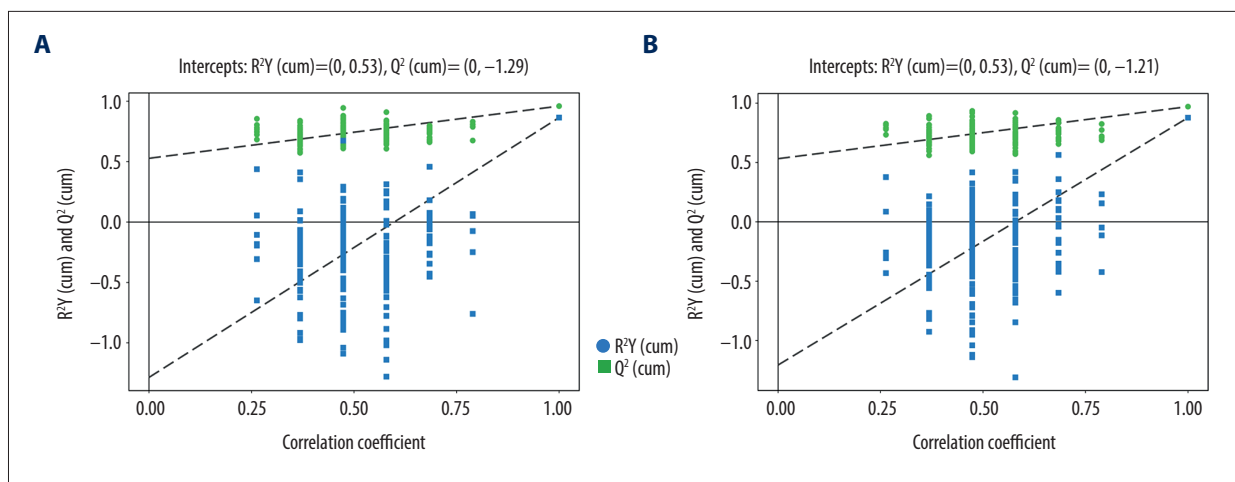


**Figure 6.** Permutation test of OPLS-DA model for group ET (EtOH) vs. Con (Control) in POS (A) and NEG (B).

**Table 1.** Differential metabolite screening tables for POS (A) and NEG (B).

(A) POS differential metabolite screening table.

ID	18	25	87	95	127	221	227
MS2 name	Crotonic acid	2-Amino-2-methyl-1,3-propanediol	gamma-Aminobutyric acid	4-Hydroxybutanoic acid lactone	Phenol	Quinone	ND
MS2 score	0.6122	0.837	0.8433	0.9642	0.8668	0.6954	ND
VIP	1.123579948	1.247014417	1.388431352	1.395961643	1.416543877	1.476595624	1.130405806
P value	0.014044416	0.004626831	0.00082763	0.001002588	0.000763936	0.000309697	0.02633426
Fold change	1.246337969	0.686732157	1.354834933	1.395307351	0.559062523	0.504541479	1.225435028
Log fold change	0.317695337	-0.542180574	0.438117091	0.480582946	-0.83891846	-0.986955215	0.293293995

(B) NEG differential metabolite screening table.

ID	52	55	74	97	147	157	183
MS2 name	Acetohydroxamic acid	Glycine	ND	ND	ND	ND	DL-lactate
MS2 score	0.9988	0.969	ND	ND	ND	ND	0.984
VIP	1.077682513	1.048769476	1.142137125	1.412005296	1.341073862	1.54065849	1.372786314
P value	0.004080437	0.007713166	0.045876493	2.72877E-05	0.001973899	4.0515E-06	4.68747E-06
Fold change	0.644126319	0.808958572	0.646075067	0.740130322	0.360025508	0.225435636	0.422824573
Log fold change	-0.634584454	-0.305862273	-0.630226294	-0.434148772	-1.473828969	-2.149212508	-1.241868871

POS – positive ion mode; NEG – negative ion mode; ND – not determined. Differential metabolite screening tables for POS (A) and NEG (B). ID – the unique number of the substance obtained in this qualitative match; MS2 name – the name of the substance's secondary match; MS2 score – the score of the second-level match of the substance, the value [0, 1], the larger the better; VIP – from OPLS-DA The VIP value of the model; P value – P value from t test; Fold change – the ratio of the 2 groups of experimental substances; Log fold change – fold change takes the base 2 logarithm. The differential metabolite screening conditions are VIP greater than 1 and P value less than 0.05.

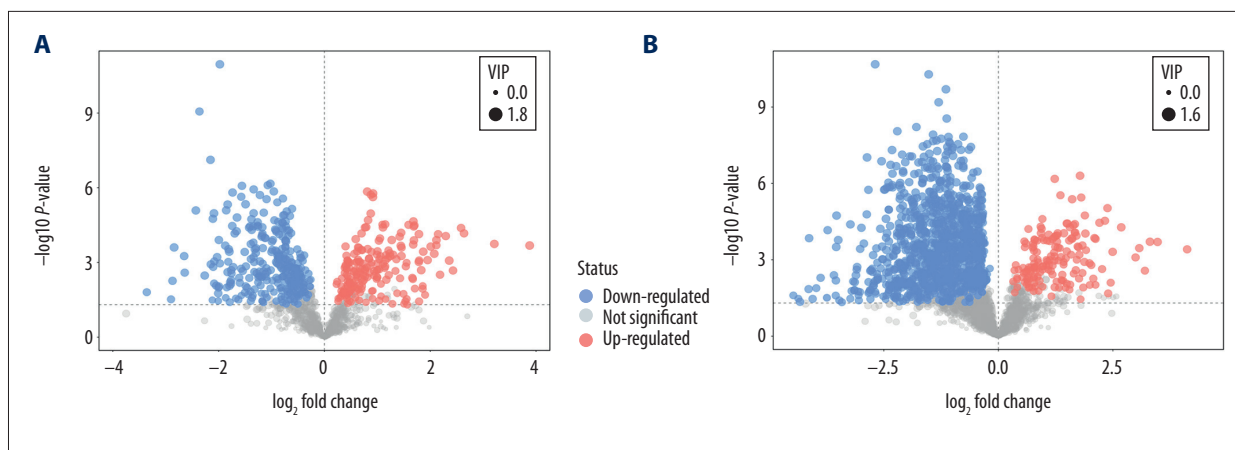


**Figure 7.** ET (EtOH) vs. Con (Control) differential metabolite screening and volcano maps in POS (A) and NEG (B). We generated VIP maps from OPLS-DA,  $VIP > 1$  and  $P < 0.05$  to determine differential metabolism that significantly contributed to clustering between groups.

T-squared ellipse) (Figure 5A, 5B). To acquire the R value and Q value for the stochastic model, the OPLS-DA model was established by the permutation test through randomly adjusting the order of the categorical variable Y (multiple times  $n=200$ ), avoiding overfitting the test model and realizing statistical significance in the evaluation model. The results of the permutation test in the experimental group and control group in the OPLS-DA model are shown in Figure 6A, 6B. The PCA and OPLS-DA models were constructed with good adaptability and predictability. The results obtained from the data detected in positive or negative ion mode demonstrated a clear separation between the control group and the experimental group, indicating significant changes in the biochemical metabolites in the liver after consuming the diet.

### Screening of differential metabolites

The multivariate statistical analysis method was performed to analyze the UHPLC/Q-TOF-MS-based metabolome data for its intrinsic characteristics. In comparison with univariate analysis, the multivariate analysis is more suitable for identifying the metabolite relationships of biological processes. Considering the results of the 2 statistical analysis methods, we can draw different conclusions from the data and help avoid false-positive errors or model overfitting caused by using only 1 type of statistical analysis [9]. In this study,  $P < 0.05$  denoted statistical significance according to the  $t$  test, and the first principal component of the OPLS-DA model had a VIP higher than 41. Examples for results of differential metabolite screening are presented in Table 1.

The screening results of the metabolites are presented in the form of a volcano plot. The results of the experimental group and the control group are shown in Figure 7A, 7B. Each point in the volcano plot demonstrated a metabolite, and the

coordinates illustrated the fold change of the group compared with each substance (by taking the base 2 logarithm), the ordinate revealed the  $P$  value of the  $t$  test (by taking the negative of the base 10 logarithm), and the scatter size indicates OPLS-DA. Based on the VIP value of the model, the scatter increased as the VIP value increased. The scatter color of red represents significantly upregulated metabolites, and that of blue and grey represent the significantly downregulated and the non-significantly different metabolites, respectively.

Systemic changes in the metabolome are caused by complex metabolic reactions and their regulation in organisms. The Kyoto Encyclopedia of Genes and Genomes (KEGG) pathway database can be used to comprehensively and systematically understand the biological processes, including changes in biological processes, traits, or disease mechanisms of drug action [10,11].

### Metabolic pathway analysis of potential markers

Further analysis of metabolic pathway is necessary because KEGG analysis can only discover the pathways in which metabolites are related, but cannot evaluate whether these pathways are intimately involved in the experimental conditions. By using a comprehensive analysis, the crucial pathways that are mostly related to metabolite differences are further identified [12].

Through matching the information of the differential metabolites, we explored the pathway database of *Mus musculus*. An example of a metabolic pathway analysis table is provided in Table 2.

The findings of metabolic pathway analysis are displayed in a bubble chart. The metabolic pathway is illustrated by the bubble in the diagram, and the size of influencing factor of the

**Table 2.** Analysis of WT and ETOH metabolic pathways in POS (A) and NEG (B).

(A) Metabolic pathway analysis example in POS.

Pathway	Total	Hits	Raw p	-ln(p)	Holm adjust	FDR	Impact	Hits Cpd
D-Glutamine and D-glutamate metabolism	5	2	0.02066	3.8795	1	1	1	L-Glutamic acid; L-Glutamine
Pyrimidine metabolism	41	5	0.042905	3.1488	1	1	0.06353	L-Glutamine; Uridine; Cytidine; Deoxycytidine; Uracil
Vitamin B6 metabolism	9	2	0.065684	2.7229	1	1	0.56863	Pyridoxal; Pyridoxamine

(B) Metabolic pathway analysis example in NEG.

Pathway	Total	Hits	Raw p	-ln(p)	Holm adjust	FDR	Impact	Hits Cpd
Purine metabolism	68	15	0.00005984	9.7238	0.0049069	0.0049069	0.24208	Xanthine; D-Ribulose 5-phosphate; L-Glutamine; AICAR; Cyclic AMP; Adenosine monophosphate; Adenylsuccinic acid; Adenosine; Xanthosine; Guanosine monophosphate; Inosine; Uric acid; Guanosine; Adenosine diphosphate ribose; Adenine
Pentose phosphate pathway	19	5	0.0098088	4.6245	0.79451	0.2381	0.34309	Deoxyribose; D-Ribulose 5-phosphate; D-Ribose; D-Ribulose 5-phosphate; Gluconolactone
Cysteine and methionine metabolism	27	6	0.01125	4.4874	0.89999	0.2381	0.16284	5'-Methylthioadenosine; L-Serine; L-Methionine; Cysteic acid; L-Cystine; 3-Sulfinolalanine

POS – positive ion mode; NEG – negative ion mode. Pathway – the name of the metabolic pathway; Total – the number of all metabolites in the pathway; Hits – the number of differential metabolites that hit this pathway; Raw p – P value obtained by enrichment analysis; -ln(p) – the P value takes the negative natural logarithm; Holm adjust – the P value corrected by the multiple hypothesis test by the Holm-Bonferroni method; FDR – P value corrected by multiple hypothesis test by false discovery rate (FDR) method; Impact – the impact factor obtained by topological analysis; Hits Cpd – the name of the differential metabolite that hits the pathway and its KEGG ID.

pathway is demonstrated by the abscissa and bubble size. In addition, the P value of enrichment analysis is indicated by the ordinate and color of the bubble (by taking the negative natural logarithm, i.e., -lnP-value), meaning that deeper colors reflect smaller P values and more significant enrichment (Figure 8).

## Discussion

ALD is one of the most prevalent diseases worldwide and can develop to hepatitis and fibrosis/cirrhosis and eventually lead to hepatocellular carcinoma (HCC) [13]. ALD is a major disease that leads to serious disease-related morbidity and mortality.

Histopathological examinations revealed significant lesions in the microscopic histology of H&E-stained liver sections in the model group [4]. The present study utilized UHPLC/Q-TOF-MS technology to analyze the livers of mice with acute alcoholic liver injury. Potential biomarkers related to alcoholic liver damage were identified through the ANOVA/OPLS-DA model. The 6 most likely related pathways were obtained through the KEGG database and META analysis, which comprised D-glutamine and D-glutamate metabolism, pyrimidine metabolism, vitamin B6 metabolism in positive ion mode (POS), purine metabolism, the pentose phosphate pathway, and cysteine and methionine metabolism in negative ion mode (NEG). The changes in the content of these endogenous metabolites reflect to some



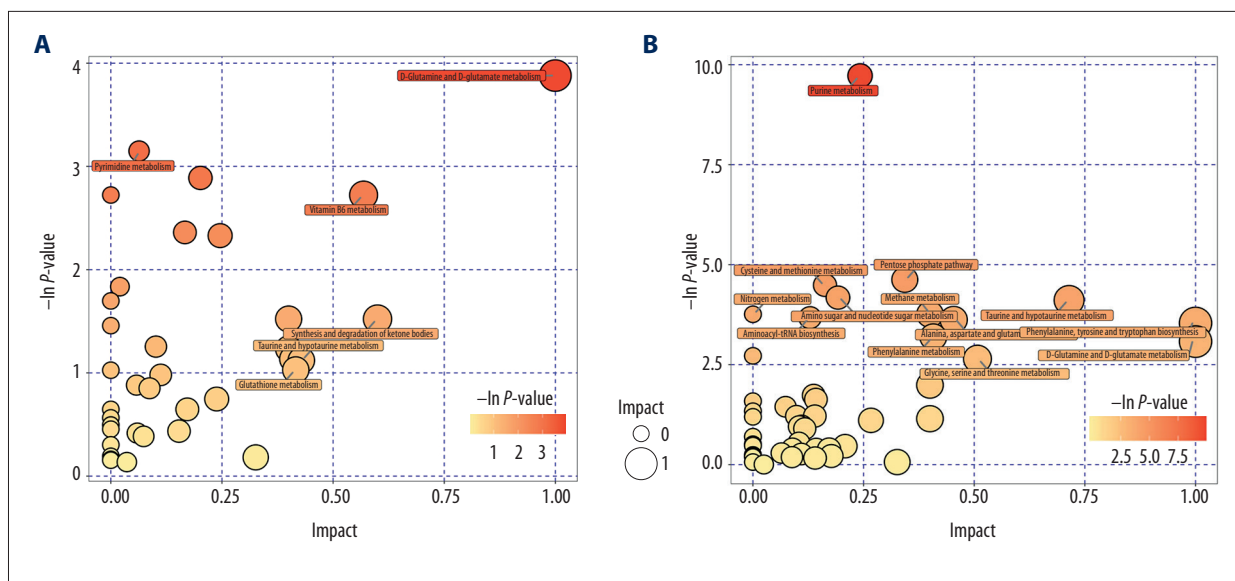


**Figure 8.** Metabolic pathway analysis of differential metabolites in POS (A) and NEG (B).

extent the changes in metabolic levels in mice after liver injury caused by alcohol. These finding could help predict the occurrence of ALD and provide a basis for monitoring changes in metabolites in the body under disease conditions.

Previous studies have revealed that vitamin B6 deficiency is associated with many adverse health effects [14]. As early as 45 years ago, Leevy et al. in the United States investigated 140 ALD patients and found that 60% of patients had low serum vitamin B6 levels, suggesting an association between vitamin B6 deficiency and ALD [15]. Approximately two-thirds of chronic alcoholics suffer from vitamin B6 deficiency, and their overall level is significantly lower than normal [16]. A bone marrow study of hospitalized patients with chronic alcoholism found that iron granulocytic anaemia is a major clinical manifestation of vitamin B6 deficiency in 23% of alcoholic patients [17]. Increasing studies have revealed that vitamin B6 circulates in the form of protein-bound pyridoxal phosphate, and the acetaldehyde products of alcohol metabolism degrading the compound are the major cause of vitamin B6 deficiency [18,19]. Folic acid, vitamin B12, and vitamin B6 are crucial cofactors in the metabolism of homocysteine, and they have been verified to effectively attenuate the increased homocysteine levels [20–23].

Homocysteine, an essential amino acid, is derived from the conversion of methionine to cysteine, and its metabolized pathways includes remethylation and transulphuration, in which homocysteine is reconverted to methionine and cysteine, respectively [24]. Therefore, supplementation with folic acid, vitamin B12, and B6 might effectively reduce the mortality of cardiovascular diseases – the ‘homocysteine hypothesis’ [20]. Studies have revealed that through interfering with the

metabolism of folate, alcohol intake exacerbated the elevated serum homocysteine levels, and was closely related to the occurrence of multiple liver diseases [25]. Additionally, patients with chronic liver diseases, as well as alcoholics, showed elevated serum levels of homocysteine independent of steatosis stage, mild fibrosis, or severe cirrhosis [26]. Decreased uric acid excretion or purine (C5H5N4) metabolic disorders caused by increased uric acid in the body cause great pain and various complications in humans, and the content of purines in beer is high. Numerous studies have shown a correlation between beer intake and the occurrence of gout [27,28]. The pentose phosphate pathway (PPP) is the first step in glycolysis and is a branch of sugar metabolism produced after the production of glucose-6-phosphate (G6P). Increasing evidence shows that the role of PPP in cells is not only to provide ribose as a raw material for DNA synthesis, but also to generate NADPH, which is an important hydrogen donor for the synthesis of biological macromolecules. In contrast, maintaining intracellular redox balance is perhaps the most important role of NADPH [29]. In the oxidative equilibrium of liver cells, reactive oxygen species (ROS) and reactive nitrogen species (RNS) are normal cell metabolites and have beneficial effects in cells. If the production of active oxygen clusters is excessive, oxidative stress will occur. Oxidative stress is a key factor in the formation of ALD [30,31]. PPP is also related to inflammatory responses. By controlling this metabolic pathway, it is possible to intervene in the signal transduction of active molecules that exert a key role in the immune response [32].

Furthermore, the liver is one of the most important metabolic organs in the body, and chemical liver injury is an important initiating link that triggers a variety of liver diseases. Therefore, research on the pathogenesis of chemical liver

injury is of great significance for the prevention and therapy of chronic liver disease. Animal experimentation is the only way to study the pathogenesis of chemically induced acute liver injury. In studying the pathogenesis of liver diseases and anti-hepatic drugs, it is very important to use metabolomics technology to select scientifically valid, practical, and repetitive liver damage biomarkers, which can provide a scientific basis for clinical diagnosis.

## References:

- Gao B, Bataller R: Alcoholic liver disease: Pathogenesis and new therapeutic targets. *Gastroenterology*, 2011; 141: 1572–85
- Diehl AM: Liver disease in alcohol abusers: Clinical perspective. *Alcohol*, 2002; 27: 7–11
- Zhang Y, Ye QF, Lu L et al: Panax notoginseng saponins preconditioning protects rat liver grafts from ischemia/reperfusion injury via an antiapoptotic pathway. *Hepatobiliary Pancreat Dis Int*, 2005; 4: 207–12
- Fang H, Zhang AH, Sun H et al: High-throughput metabolomics screen coupled with multivariate statistical analysis identifies therapeutic targets in alcoholic liver disease rats using liquid chromatography-mass spectrometry. *J Chromatogr B Analyt Technol Biomed Life Sci*, 2019; 1109: 112–20
- Deda O, Virgiliou C, Orfanidis A et al: Study of fecal and urinary metabolite perturbations induced by chronic ethanol treatment in mice by UHPLC-MS/MS targeted profiling. *Metabolites*, 2019; 9: pii: E232
- Bertola A, Mathews S, Ki SH et al: Mouse model of chronic and binge ethanol feeding (the NIAAA model). *Nat Protoc*, 2013; 8: 627–37
- Acanski MM, Vujic DN: Comparing sugar components of cereal and pseudocereal flour by GC-MS analysis. *Food Chem*, 2014; 145: 743–48
- Bylesjo M, Eriksson D, Sjodin A et al: Orthogonal projections to latent structures as a strategy for microarray data normalization. *BMC Bioinformatics*, 2007; 8: 207
- Nahum LH: Reflections on obesity. 1964. *Conn Med*, 2014; 78: 561–62
- Kanehisa M, Goto S: KEGG: Kyoto Encyclopedia of Genes and Genomes. *Nucleic Acids Res*, 2000; 28: 27–30
- Kanehisa M, Sato Y, Kawashima M et al: KEGG as a reference resource for gene and protein annotation. *Nucleic Acids Res*, 2016; 44: D457–62
- Xia J, Sinelnikov IV, Han B et al: MetaboAnalyst 3.0 – making metabolomics more meaningful. *Nucleic Acids Res*, 2015; 43: W251–57
- Alpert L, Hart J: The pathology of alcoholic liver disease. *Clin Liver Dis*, 2016; 20: 473–89
- Liu Z, Li P, Zhao ZH et al: Vitamin B6 prevents endothelial dysfunction, insulin resistance, and hepatic lipid accumulation in Apoe (–/–) mice fed with high-fat diet. *J Diabetes Res*, 2016; 2016: 1748065
- Leevy CM, Cardi L, Frank O et al: Incidence and significance of hypovitaminemia in a randomly selected municipal hospital population. *Am J Clin Nutr*, 1965; 17: 259–71
- Cravo ML, Camilo ME: Hyperhomocysteinemia in chronic alcoholism: Relations to folic acid and vitamins B(6) and B(12) status. *Nutrition*, 2000; 16: 296–302
- Savage D, Lindenbaum J: Anemia in alcoholics. *Medicine (Baltimore)*, 1986; 65: 322–38
- Labadarios D, Rossouw JE, McConnell JB et al: Vitamin B6 deficiency in chronic liver disease – evidence for increased degradation of pyridoxal-5'-phosphate. *Gut*, 1977; 18: 23–27
- Lumeng L: The role of acetaldehyde in mediating the deleterious effect of ethanol on pyridoxal 5'-phosphate metabolism. *J Clin Invest*, 1978; 62: 286–93
- Clarke R, Armitage J: Vitamin supplements and cardiovascular risk: Review of the randomized trials of homocysteine-lowering vitamin supplements. *Semin Thromb Hemost*, 2000; 26: 341–48
- Ntaios GC, Savopoulos CG, Chatziz Nikolaou AC et al: Vitamins and stroke: The homocysteine hypothesis still in doubt. *Neurologist*, 2008; 14: 2–4
- Thambyrajah J, Landray MJ, Jones HJ et al: A randomized double-blind placebo-controlled trial of the effect of homocysteine-lowering therapy with folic acid on endothelial function in patients with coronary artery disease. *J Am Coll Cardiol*, 2001; 37: 1858–63
- van Oort FV, Melse-Boonstra A, Brouwer IA et al: Folic acid and reduction of plasma homocysteine concentrations in older adults: A dose-response study. *Am J Clin Nutr*, 2003; 77: 1318–23
- Ntaios G, Savopoulos C, Grekas D et al: The controversial role of B-vitamins in cardiovascular risk: An update. *Arch Cardiovasc Dis*, 2009; 102: 847–54
- Perry DJ: Hyperhomocysteinemia. *Baillieres Best Pract Res Clin Haematol*, 1999; 12: 451–77
- Remkova A, Remko M: Homocysteine and endothelial markers are increased in patients with chronic liver diseases. *Eur J Intern Med*, 2009; 20: 482–86
- Choi HK, Atkinson K, Karlson EW et al: Alcohol intake and risk of incident gout in men: A prospective study. *Lancet*, 2004; 363: 1277–81
- Makinouchi T, Sakata K, Oishi M et al: Benchmark dose of alcohol consumption for development of hyperuricemia in Japanese male workers: An 8-year cohort study. *Alcohol*, 2016; 56: 9–14
- Cairns RA, Harris IS, Mak TW: Regulation of cancer cell metabolism. *Nat Rev Cancer*, 2011; 11: 85–95
- Shaw S, Jayatilake E, Ross WA et al: Ethanol-induced lipid peroxidation: Potentiation by long-term alcohol feeding and attenuation by methionine. *J Lab Clin Med*, 1981; 98: 417–24
- Arteel GE: Oxidants and antioxidants in alcohol-induced liver disease. *Gastroenterology*, 2003; 124: 778–90
- Ham M, Choe SS, Shin KC et al: Glucose-6-phosphate dehydrogenase deficiency improves insulin resistance with reduced adipose tissue inflammation in obesity. *Diabetes*, 2016; 65: 2624–38

## Conclusions

In this study, we revealed 3 major differential metabolic pathways in positive and negative ion channels in a mouse model of ALD, and identified several potential biomarkers. However, the exact role of these differential metabolic pathways in ALD remains to be further explored.

## Conflict of interest

None.